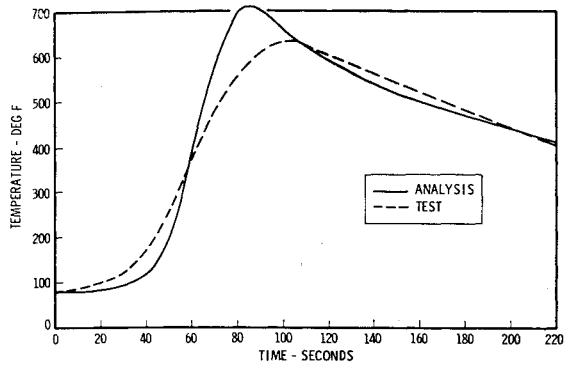

Fig. 3 Test specimen back-face temperature history.

Some of the effects of compression due to sewing can be seen by comparison of the maximum temperature on samples 1 and 4. What is not indicated is the temperature at or near the threads, where more than average compression occurs; on some samples these areas were found to be as much as 400°F hotter than the temperatures midway between the threads.

In general it has been found advisable to sew the material with as little local compression in the thread area as possible. This precaution results both in reduced temperatures in the thread area and better wear resistance of the material.

The effect of increasing the nominal Fiberfrax thickness results in a decrease in the temperature of the back surface, as seen by comparison of temperatures on samples 6, 7, and 10.

Analysis

Proper applications of the material require an analytical model with which the temperature behavior of the material in use can be predicted with some confidence. In this instance, the analytical model considered a heat source to the front face of the test sample of a value determined by the calorimeter measurement. The level of the heat source is reduced by the absorptivity[3] of the quartz cloth at 0.95 μ wave length 0.585. The front face is assumed to radiate with emissivity[4] 0.68 and convect to the surroundings at a constant nominal temperature. Likewise, the back face is assumed to radiate, with emissivity 0.92, and convect to the same environment as the front face. The point is that it is important to account for spectral variations in surface radiation properties and that the published surface properties of pure quartz fit the behavior of the Astroquartz satisfactorily. Standard finite-difference techniques were applied to the transient heat conduction equation for the thermal history prediction of the blanket. A comparison of analytical and test results appears in Fig. 3. The peak temperatures are predicted within 10% based on temperature rise, and the final temperatures are predicted within 10 deg.

Conclusions

The low-density sandwich of quartz cloth and Fiberfrax filler is an excellent heat shield for high radiative heating rate applications, especially where flexing is necessary during heating. Generally, it is recommended that the surface be kept clean of any "protective" coatings, such as silicone rubber, since such materials may have a detrimental effect on the heat shield performance (see charred sample, Fig. 4). Optimum material performance is obtained when stitching is kept as loose as practicable.

Flight evaluation of the heat shield (Fig. 1) will be conducted shortly on a Thor-boosted Delta vehicle. In-flight temperature measurements will be made, and the results of the measurements will be reported in a subsequent article.

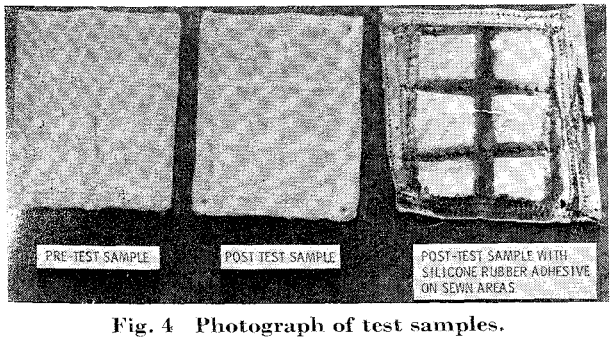

Fig. 4 Photograph of test samples.

References

[1] Property Bulletin 310-30, Industrial Glass Fabrics Department, J. P. Stevens and Co. Inc.

[2] "Refractory Fibrous Materials, Fiberfrax Specification," DS-5R 1064, March 1966, The Carborundum Co., Refractories Div.

[3] Hodgman, C. D., *Handbook of Chemistry and Physics*, Chemical Rubber Publishing Co., Cleveland, 1959.

[4] Gubareff, G. G., Janssen, J. R., and Torborg, R. H., *Thermal Radiation Properties Survey*, Minneapolis, Honeywell Research Center, 1960.

Helium Injection to Reduce Resonant Frequencies in Propellant Lines

Brantley R. Hanks* and David G. Stephens†
NASA Langley Research Center,
Langley Station, Hampton, Va.

LIQUID propellant launch vehicles often encounter severe longitudinal oscillations (accordianlike or "pogo" motion) during flight as a result of a closed-loop coupling of vibrations in the structure, propellant feed system, and engine.[1,2] One proposed "fix" is to alter the resonant frequencies of the propellant feed system by injecting small amounts of gas into the flowing liquid to decrease the speed of sound in the liquid. The lowering of sound velocity by gas bubbles in a liquid has been reported by others.[3,4] The objective of the program discussed herein was to study the change in resonant frequencies and resonant pressure responses resulting from the addition of helium to water flow lines in both normal and increased acceleration fields.

Apparatus, Test Procedure, and Analysis

The test apparatus (Figs. 1 and 2) consisted of an overhead 3-ft-diam, 8-ft-high pressurized water tank on a nonrotating foundation with a feed line running through a rotary gland and flexible rubber feed pipe to a test section mounted radially on a whirl table. The whirl table was used to produce a nominal 3.4g acceleration field on the test section to simulate a typical flight acceleration condition. The test section was a 17-ft-long, 1.5-in.-i.d., 2-in.-o.d., stainless-steel tube that had a 3-in.-diam cylinder and piston attached at its near end at the center of the whirl table. The piston was driven by a hydraulic shaker which was controlled to sweep frequency at a uniform (1 decade/min) rate at constant acceleration for frequencies above 20 Hz and at constant amplitude below 20 Hz. Water flowed into the test section from the tank above through a Y-joint just ahead of the piston

Presented at the AIAA Structural Dynamics and Aeroelasticity Specialist Conference, New Orleans, La., April 16–17, 1969 (no paper number; published in bound volume of conference papers); submitted May 16, 1969; revision received July 22, 1969.

* Aerospace Engineer. Associate AIAA.
† Head, Environmental Systems Section. Member AIAA.

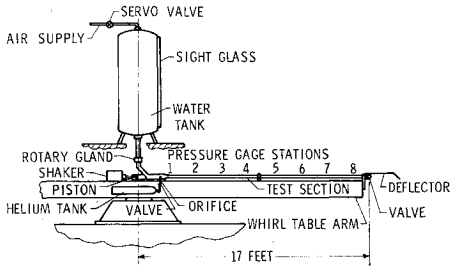

Fig. 1 Schematic of test apparatus.

and discharged through a 1.0-in.-diam, sharp-edged orifice at the end of the test section. Water supply pressure was held constant (by an automatic control system) at 40 psig at the bottom of the tank. The water flow rate was monitored visually using a sight glass and stopwatch. A tank on the whirl table supplied He through a pressure regulator to the He injection valve (a calibrated, variable-area orifice), which maintained a constant flow rate of He into the water just past the Y-joint. Quick-opening valves on the end of the steel tube and in the He line were used to initiate flow once the desired whirl table speed and ullage pressure were obtained. Pressures in the tube were monitored by diaphragm-type pressure gages at 2-ft intervals along the length and were recorded on a light beam oscillograph.

The test procedure was as follows: the tank was filled to a desired level with water; the automatically controlled ullage pressure was applied; the whirl table was brought up to 33 rpm for the $3.4g$ acceleration level; water and He flows were initiated; and the shaker was started. The pressure histories (oscillograms) were analyzed to determine the frequencies, mode shapes, and amplitudes of the dominant resonances of the liquid in the feed line test section.

The acoustic velocity C in a liquid-gas mixture in a pipe is given by[3]

$$C = \{x^2/C_g^2 + (1 - x)^2/C_l^2 + x(1 - x) \times [\rho_l/P_A\gamma + \rho_g K_l] + D/tE[(1 - x)\rho_l + x\rho_g]\}^{-1/2} \quad (1)$$

for adiabatic bubble expansion and contraction and by

$$C = \{\gamma x^2/C_g^2 + (1 - x)^2/C_l^2 + (1 - x) \times [\rho_l/P_A + \rho_g K_l] + D/tE[(1 - x)\rho_l + \rho_g]\}^{-1/2} \quad (2)$$

for isothermal expansion and compression of the bubbles, where x is the volume fraction of gas, C_g and C_l are the acoustic velocities in the gas and liquid, respectively; ρ_g and ρ_l are corresponding densities; P_A is the absolute pressure in test section; γ is the ratio of specific heats for the gas; K_l is the compressibility of the liquid; and D, t, and E are the inside diameter, wall thickness, and modulus of elasticity of the test section, respectively.

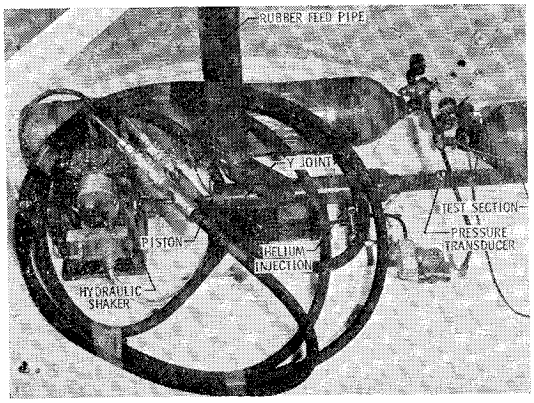

Fig. 2 Vibration input and helium injection equipment.

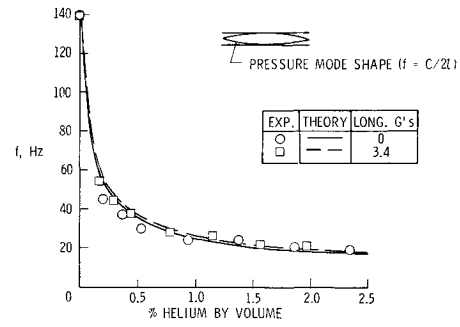

Fig. 3 Effect of helium and acceleration on frequency of dominant mode.

Both Eqs. (1) and (2) reduce to

$$C = [C_l^{-2} + (D\rho_l/tE)]^{-1/2} \quad (3)$$

for the case of no gas in the liquid.

For cases where an induced acceleration field was applied by the whirl table, P_A and x varied slightly along the test section length; calculations for these cases were based upon mean pressures and volumes.

Results and Discussions

The effects of helium volume fraction x and acceleration (0 or $3.4g$) on the dominant resonant frequency f of the fluid in the test section is shown in Fig. 3. The response of this mode ($f = C/2l$, where l is test section length, 17 ft) was very strong and easily measured, whereas the responses associated with other modes detected ($f = C/l$ and $f = C/4l$, not shown) were of much lower magnitude. The curves represent behavior as given by Eq. (1). The percentage reduction in frequency as a function of He content was found experimentally to be independent of the mode shape. The effect of the $3.4g$ longitudinal acceleration is relatively small.

The response pressure in these tests was measured in terms of a magnification factor X that is defined as the ratio of the average peak pressure at first mode resonance to the pressure in the line with no standing waves present. For water, $X \cong 10$. The effect of He on the response pressure in nondimensional form (ratio of X for the helium-water mixtures to that of water) is shown in Fig. 4a. One-half percent helium lowers the X ratio to 0.2. Also presented in Fig. 4a is a curve of the ratio of sound velocity in the helium-water mixture to that in water as calculated using Eq. (1). The X ratio appears to vary in the same manner and proportions as the C ratio. It is shown in Ref. 5 that damping of pressure waves in fluids due to the presence of gas bubbles results only at frequencies very near the resonant frequencies of the bubbles. The resonant frequency of a bubble in a liquid is

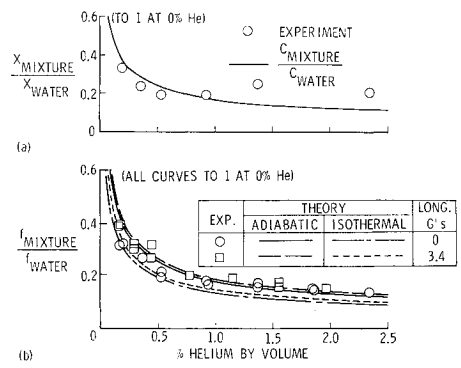

Fig. 4 a) Reduction of resonant pressure response with helium for dominant mode, and b) comparison of adiabatic and isothermal theory with frequency data for all modes.

given by[3,4]

$$f = (1/\pi d)(3P_A k/\rho_l)^{1/2} \quad (4)$$

where d is the bubble diameter. For our test conditions, Eq. (4) becomes approximately

$$f = 530/d \quad (5)$$

where d is in inches. Because the bubbles were very small‡ their resonant frequencies were well out of the test frequency range, and they probably contributed very little damping to the system. A more likely explanation for the lower X ratio at resonance is that the damping due to viscous shear and structural relaxation in the water was higher at the lower natural frequency of the mixture. The damping from these sources is[6]

$$\alpha = (\tfrac{4}{3}\eta + \eta')\omega^2/2\rho C^3 \quad (6)$$

where α is the theoretical coefficient of attenuation of acoustic waves, ω is the circular frequency of excitation, ρ and C are the density and sound velocity of the liquid, and η and η' are the shear and volume coefficients of viscosity. Since, in these tests, the frequency ω at which the magnification was measured was directly proportional to C, Eq. (6) can be written for resonant conditions as

$$\alpha \propto (\tfrac{4}{3}\eta + \eta')/\rho C \quad (7)$$

Thus, if the physical constants are approximately the same in the mixture as in the homogeneous fluid, the damping at resonance is inversely proportional to the speed of sound, and higher damping would be expected in the helium-water mixture.

There is some question as to whether the expansion and contraction of the bubbles should be treated analytically as an adiabatic or an isothermal process. Curves for adiabatic theory, Eq. (1), were shown in Figs. 3 and 4a. Figure 4b shows a nondimensional comparison of all frequency data with both adiabatic and isothermal theory, Eq. (2). The adiabatic theory appears to fit the data slightly better than the isothermal theory.

The effect of flow-pipe test section flexibility was not studied experimentally. Calculations based on Eq. (1) indicate that the flexibility of the test section was negligible in these experiments. However, Eq. (1) indicates that in the case of a very flexible pipe (such as might be the case for a launch vehicle propellant line) the speed of sound in the pipe is lowered and the effect of helium on the natural frequencies may be somewhat less than in the rigid pipe case. For example, had the test section wall thickness been 0.025 in. instead of 0.25 in., the first natural frequency would have been 114 Hz instead of 140 Hz. One percent of helium would have lowered this frequency by a factor of 4.7 instead of the factor of 5.6 for the rigid pipe case. Increasing the pipe diameter by a factor of 10 would have a similar effect.

References

[1] Rubin, S., "Longitudinal Instability of Liquid Rockets Due to Propulsion Feedback," *Journal of Spacecraft and Rockets*, Vol. 3, No. 8, Aug. 1966, pp. 1188–1195.

[2] McKenna, K. J., Walker, J. H., and Winje, R. A., "Engine-Airframe Coupling in Liquid Rocket Systems," *Journal of Spacecraft and Rockets*, Vol. 2, No. 2, March–April 1965, pp. 254–256.

[3] Karplus, H. B., "The Velocity of Sound in a Liquid Containing Gas Bubbles," Project A-097, Atomic Energy Commission Contract AF(11-1)-528, June 1958, Armour Research Foundation.

[4] Carstensen, E. L. and Foldy, L. L., "Propagation of Sound Through a Liquid Containing Bubbles," *Journal of the Acoustical Society of America*, Vol. 19, 1947, pp. 481–501.

[5] Laird, D. T. and Kendig, P. M., "Attenuation of Sound in Water Containing Air Bubbles," *Journal of the Acoustical Society of America*, Vol. 24, 1952, pp. 29–32.

[6] Kinsler, L. E. and Frey, A. R., *Fundamentals of Acoustics*, 2nd ed., Wiley, New York, 1962.

‡ Several tests were conducted using two transparent sections in the flow line. Motion pictures at 400 frames/sec showed the helium bubbles to be small and evenly distributed in the water, both at $0g$ and $3.4g$.

Burning Characteristics of Composite Solid Propellants at High Pressures

CHARLES HAFF* AND EUGENE GARNER†
Talley Industries Inc., Mesa, Ariz.

Nomenclature

K_n = area ratio
r_b = burning rate, m/sec
p_c = chamber pressure, psia
C/F = oxidizer granulation ratio, coarse to fine

Introduction

THE usual practice for designing rocket motors for operation at higher pressures is to utilize data obtained from subscale test firings at lower pressures. The data are presented on burning rate (r_b) and K_n plots and are extrapolated to the pressures required for the application. Since most design requirements are at pressures of 3000 psi and lower, experience to date has been satisfactory. Newer applications of propellant systems have dictated that the extrapolations must be reliable to the 5000 to 10,000 psi range. Most propellant systems fail to perform as expected in this region.

This Note describes a series of evaluations performed on "standard" solid propellants and presents some conclusions based on the systems investigated. Burning instability for the purpose of this Note shall be considered as any marked change in K_n slope. The condition of resonant burning or other forms of instability are not considered to be meaningful in the configurations studied.

The propellants chosen for initial evaluation, first six groups in Table 1, are standard formulations and constitute

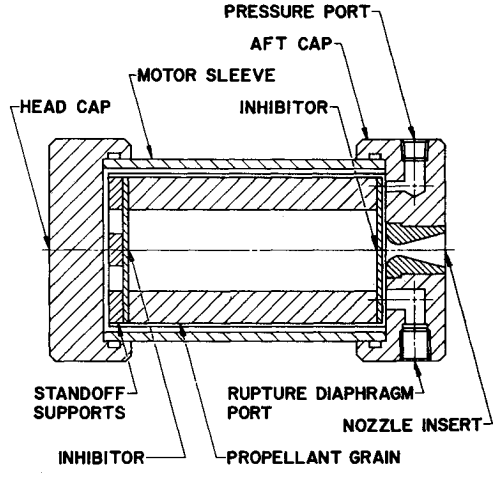

Fig. 1 K_n motor assembly test fixture.

Presented as Paper 69-438 at the AIAA 5th Propulsion Joint Specialist Conference, U. S. Air Force Academy, Colo., June 9–13, 1969; submitted June 4, 1969; revision received July 31, 1969.

* Head, Applied Research Division. Member AIAA.
† Staff Chemist.